


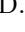





## Dilepton production from moaton quasiparticles

Zohar Nussinov <sup>1,2,\*</sup> Michael C. Ogilvie <sup>1,†</sup> Laurin Pannullo <sup>3,‡</sup> Robert D. Pisarski <sup>4,§</sup> Fabian Rennecke <sup>5,6,¶</sup> Stella T. Schindler <sup>7,8,\*\*</sup> and Marc Winstel <sup>9,††</sup>

<sup>1</sup>*Physics Department, Washington University, St. Louis, MO 63130, USA*

<sup>2</sup>*Rudolf Peierls Centre for Theoretical Physics, University of Oxford, Oxford OX1 3PU, United Kingdom*

<sup>3</sup>*Fakultät für Physik, Universität Bielefeld, D-33615 Bielefeld, Germany*

<sup>4</sup>*Department of Physics, Brookhaven National Laboratory, Upton, NY 11973*

<sup>5</sup>*Institute for Theoretical Physics, Justus Liebig University Giessen, 35392 Giessen, Germany*

<sup>6</sup>*Helmholtz Research Academy Hesse for FAIR (HFHF), Campus Giessen, Giessen, Germany*

<sup>7</sup>*Theoretical Division, Los Alamos National Laboratory, Los Alamos, NM 87545, USA*

<sup>8</sup>*Center for Theoretical Physics, Massachusetts Institute of Technology, Cambridge, MA 02139, USA*

<sup>9</sup>*Institut für Theoretische Physik, J. W. Goethe-Universität, D-60438 Frankfurt am Main, Germany*

The phase diagram of QCD may contain a moat regime in a large region of temperature  $T$  and chemical potential  $\mu \neq 0$ . A moat regime is characterized by quasiparticle *moatons* (pions) whose energy is minimal at nonzero spatial momentum. At  $\mu \neq 0$ , higher mass dimension operators play a critical role in a moat regime. At dimension six, there are nine possible gauge invariant couplings between scalars and photons. For back-to-back dilepton production, only one operator contributes, which significantly enhances production near a moat threshold. This enhancement is an experimental signature of moatons.

The phase diagram of Quantum Chromodynamics (QCD) at a nonzero temperature  $T$  and quark chemical potential  $\mu$  (or baryon chemical potential  $\mu_B = 3\mu$ ), is important for a variety of physical systems, from neutron stars, to heavy ion collisions, to the early universe. We know much about the region of  $T \neq 0$  at low  $\mu \ll T$  from heavy ion colliders operating at ultra-relativistic energies, such as the Relativistic Heavy Ion Collider (RHIC) at BNL and the Large Hadron Collider at CERN. We also have a wealth of understanding of  $\mu = 0$  behavior from first-principles lattice QCD techniques, which indicate that the chiral transition is crossover at a temperature  $T \approx 156.5 \pm 1.5$  MeV [1, 2]. However, the lattice cannot reach beyond  $\mu \sim T$  on classical computers due to the sign problem. A first-principles understanding of heavy ion collisions at moderate energies requires studying QCD at  $\mu > T$ , and neutron stars have large  $\mu \gg T$ .

As  $\mu$  increases, it is likely that a Critical End Point (CEP) develops, where a line of crossover transitions meets a line of first order transitions [3–7]. From direct computations in QCD using the Functional Renormalization Group (FRG) [8] and Schwinger-Dyson equations [9–11], as well as reconstructions based on lattice data [12, 13], this is estimated to occur for  $(T_\chi, \mu_\chi) \approx (100, 200)$  MeV. This lies in the region  $\sqrt{s}/A : 3 \rightarrow 7$  GeV in heavy ion collisions. By perverse coincidence, the Beam Energy Scan by the STAR experiment at RHIC studied collisions

down to  $\sqrt{s}/A = 7$  GeV, and at  $\sqrt{s}/A = 3$  GeV in fixed target mode, but not in between. While intriguing, their results did not find evidence for a CEP. This region will be studied at the Nuclotron-based Ion Collider Facility (NICA) at the Joint Institute for Nuclear Research, and with the Compressed Baryon Matter (CBM) experiment at the Facility for Antiproton and Ion Research (FAIR) at the GSI Helmholtz Center for Heavy Ion Research.

The CEP, while of fundamental significance, may be difficult to probe directly. In vacuum, the mass of the  $\sigma$  meson is large, perhaps  $\sim 500$  MeV, with a width of similar order, rendering it difficult to extract experimentally. In contrast, at the CEP the  $\sigma$  is precisely massless [14] but pions remain massive. Because the  $\sigma$ 's singularity is so far from the origin in vacuum, it must travel a long way, suggesting that the basin of attraction to the CEP can be narrow. This naive argument is confirmed by studies of the chiral phase transition, where critical scaling is absent even close to the transition; see Refs. [8, 15–21].

In contrast, there can be a moat regime in the QCD phase diagram, where the dispersion relations of quark correlations in meson channels have a minimum at nonzero spatial momentum [8]. As detailed below, this is associated with exotic phases featuring spatial modulations. Crucially, the moat regime may arise in a *large* region of the phase diagram at finite  $T$  and  $\mu$ , which includes the vicinity of the CEP. Experimental observation of a moat regime would not only indicate novel phases of QCD, but could also help us home in on the location of the CEP. In this Letter, we describe signals of moats in dilepton production.

**Moat regimes at  $\mu \neq 0$ .** A natural question is whether a moat regime is an artifact of a given approximation method. Moat regimes are *ubiquitous* in condensed mat-

\* zohar@wustl.edu

† mco@wustl.edu

‡ lpanullo@physik.uni-bielefeld.de

§ pisarski@bnl.gov

¶ fabian.rennecke@theo.physik.uni-giessen.de

\*\* schindler@lanl.gov

†† winstel@itp.uni-frankfurt.de; corresponding author

ter; see Refs. [22–26] and footnote [27]. Indeed, the term “moat” hails from condensed matter [28, 29]. Furthermore, moat regimes naturally arise in theories with combined charge and complex conjugation ( $CK$ ) symmetry [30]. Because the Dirac operator is non-Hermitian at  $\mu \neq 0$ , this includes QCD [31, 32]. This is a particular case of broad non-Hermitian theories with generalized  $\mathcal{PT}$  symmetries [33–35].

Oftentimes, moat regimes onset when the wave function renormalization constant  $Z$  for the quadratic spatial momentum term becomes negative. A closely related phenomenon is the appearance of a “disorder line” [30, 32, 36], separating a region in which the two-point correlation function has exponential falloff at large distances, from a region in which it behaves as an exponential times an oscillatory function, similar to Friedel oscillations, which are screened at non-zero temperature [37]. If the dip in the moat dispersion relation is sufficiently deep, then the theory may develop a finite momentum (i.e., spatially nonuniform) condensate. Direct transitions from a spatially homogeneous broken symmetry phase to an inhomogeneous phase may arise (Fig. 1).

Moat regimes and their associated phases appear in many models sharing features with QCD. A canonical example is the Gross-Neveu model in  $(1+1)$  dimensions. This theory is asymptotically free, spontaneously breaks chiral symmetry through dynamical generation of mass, and is tractable when the number of fermions  $N \rightarrow \infty$ . The phase diagram at low  $\mu < T$  is similar to what we suspect occurs in QCD in the chiral limit: a line of second order transitions extends from  $\mu = 0$  and  $T \neq 0$ . Due to the emergence of the Peierls transition, this line ends not in a CEP but in a Lifshitz point; for lower  $T$ , there is a region with spatially inhomogeneous condensates [38–46]. Crucially, the Gross-Neveu model has a moat regime in a broad region of the  $T$ - $\mu$  plane [47] (Fig. 1).

Numerous studies have been carried out in  $(3+1)$  dimensions. In the Nambu-Jona-Lasino (NJL) model [24, 48–53], the presence of an inhomogeneous phase depends strongly upon the regularization scheme, while the occurrence of a moat regime is rather insensitive to the regularization [54]. Schwinger-Dyson analysis shows that the symmetric solution is unstable to an inhomogeneous phase at low  $T$  and high  $\mu$  [55]. Disorder lines appear in Polyakov-Nambu-Jona-Lasino (PNJL) models [56, 57], Polyakov quark-meson models [58], static quark models at strong coupling [59], liquid-gas models [60], and in four-fermion models in  $(2+1)$  dimensions [61] [62]. For scalar models with global  $O(N)$  symmetry, Goldstone bosons can disorder the system into a quantum pion liquid [63–65]. Moatons appear to be a robust feature of many models of hadronic physics at nonzero density, while inhomogeneous phases are less common.

Refs. [66, 67] showed that a moat regime affects particle production through two-particle correlations generated by thermodynamic fluctuations [67] and Hanbury Brown-Twiss interferometry for pions [68, 69]. In this Letter, we compute how quasiparticle pions in a

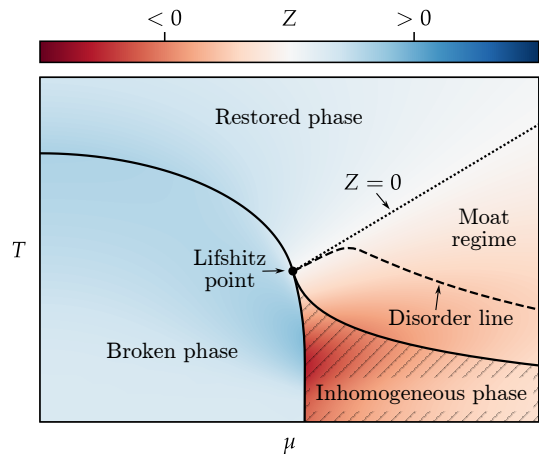


FIG. 1. A phase diagram sketch based on the Gross-Neveu model in Ref. [47]. Red shading indicates a moat regime, where  $Z < 0$ . Solid lines separate different phases. Dashed lines indicate qualitative changes in system correlations, related to spatial modulations. The exact location and nature of each transition is model dependent. However, an extensive moat regime is a common feature of models, and is also seen in FRG analyses of QCD [8]. In the Gross-Neveu model, the CEP is replaced by a Lifshitz point due to the emergence of an inhomogeneous phase.

moat regime, which we dub “moatons”, affect dilepton production. For technical reasons we limit ourselves to a dilepton pair with zero spatial momentum, and leave the more involved analysis of nonzero spatial momentum to a later publication. We note that Ref. [70] also finds enhanced production of dileptons for the specific case of a single inhomogeneous chiral spiral, and compare our approaches in the Supplemental Material.

**Effective Lagrangian for the moat regime.** A simple model of a moat is the Lagrangian [63, 64]

$$\mathcal{L} = \frac{1}{2}(\partial_0 \vec{\phi})^2 + \frac{Z}{2}(\partial_i \vec{\phi})^2 + \frac{1}{2M^2}(\partial_i^2 \vec{\phi})^2 + \frac{m^2}{2}\vec{\phi}^2 + \frac{\lambda}{4}(\vec{\phi}^2)^2. \quad (1)$$

Here,  $\vec{\phi} = (\sigma, \vec{\pi})$  represents an  $O(4)$  vector for the  $\sigma$  meson and pions. This Lagrangian is not possible in vacuum because of Lorentz invariance, but is possible when  $T, \mu \neq 0$ , as the thermal bath provides a preferred frame. To maintain causality, we insist that time derivatives only enter quadratically.

A moat regime arises in Eq. (1) when  $Z$  is negative, so the energy has a minimum at non-zero momentum. This was first observed in QCD at finite  $T$  and  $\mu$  in an FRG analysis [8]. Consequently, we must include a non-renormalizable term quartic in spatial derivatives in Eq. (1). While this term may look unfamiliar, it is natural in derivative expansions of effective Lagrangians. Examples include systems near second-order phase transitions [71] and condensed matter systems [22–26] (where such derivatives may be replaced by their discrete lat-

tice counterparts [72]) for which only Galilean invariance applies.

We cannot *a priori* drop higher mass dimension terms when constructing a full effective field theory (EFT) of a moat regime. Thus our model in Eq. (1) only caricatures an EFT about the global minimum of the dispersion relation [73], valid when  $\langle(\partial_i\vec{\phi})^2\rangle \ll M^4$  and  $\langle(\vec{\phi})^2\rangle \ll M^2$ . We cannot rule out additional local minima [74]; however, we show below that the dominant effects stem from field configurations at the global minimum, as in Refs. [66–68]. For simplicity we work in the symmetric ( $\langle\vec{\phi}\rangle = 0$ ) regime.

**Dilepton production.** At leading order in  $\alpha = e^2/4\pi$ , the dilepton production rate is proportional to the photon self energy  $\Pi^{\mu\nu}$  [75]:

$$\frac{d^4R}{dp^4} = \frac{\alpha}{12\pi^4} \frac{n(\omega)}{-P^2} \text{Im} \Pi^{\mu\mu}(p_0, \vec{p}). \quad (2)$$

Here  $\omega > 0$  with the Bose function  $n(\omega) = 1/(\exp(\omega/T) - 1)$ . We analytically continued the Euclidean energy  $p_0$  to Minkowski space,  $p_0 = -i(\omega + 0^+)$ , so  $-P^2 = \omega^2 - \vec{p}^2$ .

In vacuum, vector meson dominance implies that pion production proceeds entirely through virtual  $\rho_\mu$  mesons [76]. In heavy ion collisions, successful fits to the dilepton excess below the  $\rho_\mu$  meson peak are usually obtained by a broadened  $\rho_\mu$  in nuclear matter [77–79]. In contrast, our analysis is valid in the chirally restored phase, cf. Fig. 1. Here, we study additional contributions from moatonic pions.

We consider the possible dimension-6 terms that can contribute to dilepton production in a QCD moat regime in four dimensions, where a spin zero field  $\vec{\phi}$  carries dimensions of mass. To obey gauge invariance of couplings to the photon field ( $A_\mu$ ), we replace  $\partial_\mu \rightarrow D_\mu$  in Eq. (1),

$$\frac{1}{2}(D_0\vec{\phi})^2 + \frac{1}{2M^2}(D_i\vec{\phi})^2 + \frac{Z}{2}(D_i\vec{\phi})^2. \quad (3)$$

Additionally, there are two terms involving two derivatives and four  $\vec{\phi}$ 's, as in Eq. (2) of Ref. [64],

$$\begin{aligned} & \frac{C_1}{M^2}(D_0\vec{\phi})^2|\vec{\phi}^2| + \frac{C_2}{M^2}(D_i\vec{\phi})^2|\vec{\phi}^2| \\ & + \frac{C_3}{M^2}(\vec{\phi} \cdot D_0\vec{\phi})^2 + \frac{C_4}{M^2}(\vec{\phi} \cdot D_i\vec{\phi})^2. \end{aligned} \quad (4)$$

Since only Galilean invariance holds, the coefficients of terms involving temporal and spatial derivatives may differ. Gauge invariance requires that photons only couple through the field strength,  $F_{\mu\nu} = \partial_\mu A_\nu - \partial_\nu A_\mu$ , giving

$$\left( \frac{C_5}{M^2} F_{0i}^2 + \frac{C_6}{M^2} F_{ij}^2 \right) |\vec{\phi}^2|. \quad (5)$$

The above terms are rather mundane, but the final ones are not:

$$\frac{ieC_7}{M^2} F_{0i} [(D_0\phi)^* D_i\phi - (D_i\phi)^* D_0\phi] + \frac{ieC_8}{M^2} F_{ij} (D_i\phi)^* D_j\phi. \quad (6)$$

Charge conjugation  $\mathcal{C}$  acts as  $A_\mu \rightarrow -A_\mu$ ,  $F_{\mu\nu} \rightarrow -F_{\mu\nu}$ , and  $\phi \rightarrow \phi^*$ . Eq. (6) is thus  $\mathcal{C}$ -invariant, as  $F_{\mu\nu} = -F_{\nu\mu}$  compensates for switching  $\phi$  and  $\phi^*$  under  $\mathcal{C}$ . Eq. (6) is also invariant under time reversal  $\mathcal{T}$ , as its first two terms contain two time derivatives. These terms are real if the coupling has an overall factor  $i$ . We take these terms proportional to  $e$ , so their effects vanish as  $e \rightarrow 0$ .

Eqs. (3)-(6) represent the complete set of operators to sixth order in the mass dimension. Other terms, e.g.,  $(D_i D_j \phi)^* (D_i D_j \phi)$  and  $(D_i D_j \phi)^* (D_j D_i \phi)$ , are linear combinations of the above. We emphasize that all these new operators, including the ones in Eq. (3), are dictated by gauge symmetry. None of these have been taken into account in Ref. [70].

Next, we examine which operators in Eqs. (3)-(6) contribute to Eq. (2). Only the imaginary part of  $\Pi^{\mu\nu}$  enters Eq. (2), so we can drop the terms in Eqs. (4)-(5), as they only affect tadpole-like diagrams. The only new contribution to dilepton production is the  $|D_i^2\phi|^2$  term in Eq. (3), from the trilinear coupling between  $A_i(P)$ ,  $\phi(K)$ , and  $\phi^*(-P-K)$ . This vertex is

$$\Gamma^j(P, K) = ie(2k+p)^j \left[ Z + \frac{1}{M^2} (\vec{k}^2 + (\vec{k} + \vec{p})^2) \right]. \quad (7)$$

From Eq. (1), the (effective) pion propagator in the moat regime is

$$\begin{aligned} \Delta^{-1}(K) &= k_0^2 + Z\vec{k}^2 + \frac{(\vec{k}^2)^2}{M^2} + m^2 \\ &= k_0^2 + \frac{(\vec{k}^2 - k_M^2)^2}{M^2} + m_{\text{eff}}^2, \end{aligned} \quad (8)$$

where the moat momentum  $k_M$  satisfies  $k_M^2 = -ZM^2/2$ , and the effective mass is  $m_{\text{eff}}^2 = m^2 - Z^2M^2/4$ . A moat arises when  $Z$  is negative and  $k_M^2$  is positive.

It is readily verified that the vertex in Eq. (7) satisfies the Ward identity

$$P^\mu \Gamma^\mu(P, K) = ie [\Delta^{-1}(K+P) - \Delta^{-1}(K)]. \quad (9)$$

The Ward identity implies that the photon self-energy is always transverse,  $P^\mu \Pi^{\mu\nu}(P) = 0$ . Note that this would not be the case without the new contribution  $\sim 1/M^2$ .

To illustrate the effects of the terms in Eq. (6), we carry out computations for dilepton pair production at rest in the frame of the thermal medium, with  $\vec{p} = 0$ . Here, only spatial components  $\text{Im} \Pi^{ii}$  enter. The complete vertex  $\Gamma_7^\mu \sim C_7/M^2$  is transverse in  $P^\mu$  and does not contribute to Eq. (9). The coupling to a spatial photon is

$$\Gamma_7^i \sim \pm \frac{ieC_7}{M^2} (p_0 - 2k_0) p^0 k^i. \quad (10)$$

When  $\vec{p} = 0$ , moatons carry positive energy, so the only open channel has  $p_0 = 2k_0$  by energy conservation. This vertex vanishes. The trilinear vertex

$$\Gamma_8^i \sim \pm \frac{ieC_8}{M^2} (\vec{k} \cdot \vec{p} p^i - \vec{p}^2 k^i), \quad (11)$$

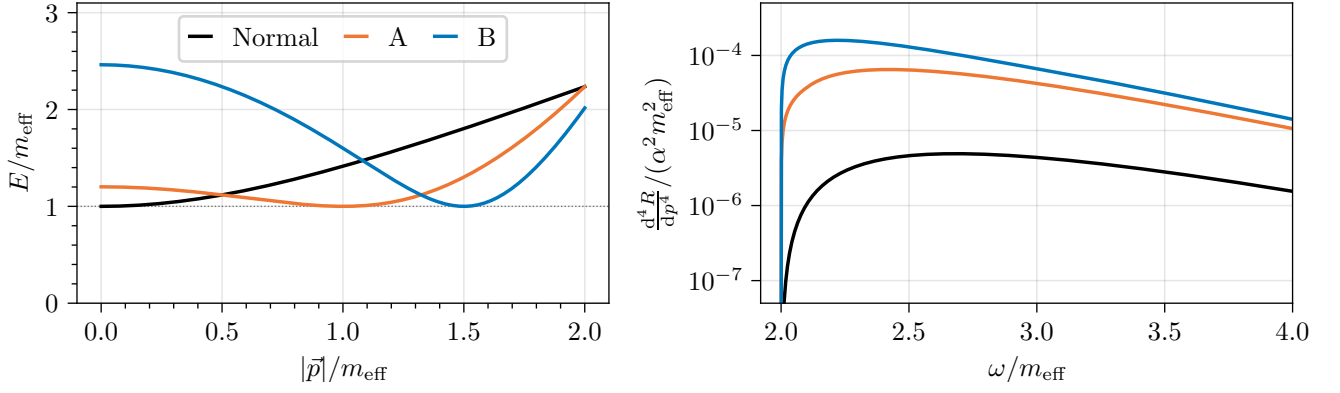


FIG. 2. (Left) Dispersion relations for various choices of  $Z$  and  $M$  in Eq. (8) and (Right) their corresponding dilepton production rate in Eq. (2) as a function of  $\omega$  at  $T = 0.5m_{\text{eff}}$ . The normal dispersion relation has  $Z = 1$ ,  $M = \infty$  and  $m_{\text{eff}} = m$ . Both pions with a shallow moat (curve A, with  $k_M/m_{\text{eff}} = 1.0$  and  $M/m_{\text{eff}} = 1.5$ ) and pions with a deep moat (curve B, with  $k_M/m_{\text{eff}} = 1.5$  and  $M/m_{\text{eff}} = 1.0$ ) enhance dilepton production. Note, however, that the value of  $m_{\text{eff}}$  does change as  $T$  and  $\mu$  vary.

is transverse in  $p^i$ , drops out of Eq. (9), and vanishes at  $\vec{p} = 0$ . However, Eqs. (10,11) do contribute when  $\vec{p} \neq 0$ . This is evident in the  $C_8$  term. For the  $C_7$  term, this is because channels with Landau damping (where  $p_0 \neq 2k_0$ ) open up.

The leading contributions to  $\text{Im } \Pi^{\mu\nu}$  come from the moaton-anti-moaton production diagram,

$$\Pi^{ii}(p_0) = e^2 T \sum_{n'} \int \frac{d^3 k}{(2\pi)^3} (\Gamma^i)^2 \Delta(P+K) \Delta(P), \quad (12)$$

where  $K = (2\pi n' T, \vec{k})$ . Evaluating the bosonic Matsubara frequency sum over  $n'$ ,

$$\begin{aligned} \text{Im } \Pi_{jj}(\omega) &= 4\alpha\theta(\omega^2 - 4m_{\text{eff}}^2) \left[ 1 + 2n\left(\frac{\omega}{2}\right) \right] \\ &\quad \times \frac{\sqrt{\omega^2 - 4m_{\text{eff}}^2}}{M\omega} \sum_{k_{\pm}} k_{\pm}^3 \theta(k_{\pm}) \end{aligned} \quad (13)$$

where

$$k_{\pm}^2 = k_M^2 \pm \frac{M\sqrt{\omega^2 - 4m_{\text{eff}}^2}}{2} \quad (14)$$

is the spatial momentum of the moatons. As the moatons are back to back, their momenta have the same magnitude. Near threshold, where  $\omega^2 \approx 4m_{\text{eff}}^2 + 0^+$ , we can approximate  $\vec{k} \approx k_M \hat{k} + \delta\vec{k}$ , where  $\hat{k}^2 = 1$ . About this point, the energy is quadratic in  $\delta\vec{k}$ ,

$$E_{\pm}(\vec{k}) \approx m_{\text{eff}} + \frac{2k_M^2}{m_{\text{eff}} M^2} (\hat{k} \cdot \delta\vec{k})^2 + \dots \quad (15)$$

For pions with a normal dispersion relation  $E^2 = k^2 + m^2$ , the photon self-energy is

$$\text{Im } \Pi_{jj} = \frac{\alpha}{2} \theta(\omega^2 - 4m^2) \left[ 1 + 2n\left(\frac{\omega}{2}\right) \right] \frac{(\omega^2 - 4m^2)^{\frac{3}{2}}}{\omega}. \quad (16)$$

The result for dilepton production from moatons, Eq. (13), obscures an interesting cancellation. For  $\vec{p} = 0$ , for

the imaginary part of the loop integral, energy momentum conservation imposes

$$\delta(\omega^2 - 4m_{\text{eff}}^2) = \frac{M^2}{2k_M^2} \frac{\delta(k - k_{\pm})}{|\hat{k} \cdot \delta\vec{k}|}, \quad (17)$$

where the numerator on the right hand side arises from the Jacobian going from a  $\delta$ -function in  $\omega$  to one in  $k$ . This factor would produce a van-Hove singularity, as arises for dilepton production from plasminos in the hard thermal loop approximation [80]. For moatons near threshold, however,

$$\Gamma^j(P, K) \approx 2iek^j \left[ \frac{4k_M}{M^2} (\hat{k} \cdot \delta\vec{k}) \right] \quad (18)$$

vanishes as  $\delta\vec{k} \rightarrow 0$ , and there is no van Hove singularity. Consequently the dilepton rate turns on smoothly at threshold.

The left panel of Fig. (2) illustrates three dispersion relations: normal, a shallow moat, and a deep moat; the right panel of Fig. (2) illustrates their corresponding dilepton production rates. While these curves have similar shapes near threshold, moatons significantly enhance dilepton production relative to normal pions. Within our studied parameter range, neither the value of  $k_M^2$  nor the difference  $E(|p|=0) - E(|p|=k_M)$  significantly alters the dilepton enhancement. Consequently, this enhancement should not depend on a quantitative determination of the moat regime from phenomenological models or the FRG.

Importantly, the value of  $m_{\text{eff}}$  depends *strongly* upon  $T$  and  $\mu$ . This variation can only be computed in an effective model, such as the FRG.

**Outlook.** We argue that QCD probably exhibits a moat regime in a broad swath of the  $T$ - $\mu$  plane. In this Letter, we showed that enhancement of dilepton production is an important signature of a moat regime. Our principal shortcoming is that we cannot predict values for parameters like  $M$  and  $Z$ , and thus  $k_M$  and  $m_{\text{eff}}$ . We expect that

$M$  is a few times  $m_\pi$ , and  $m_{\text{eff}}$  is moderately less than  $m_\pi$ . Work is in progress on extracting these parameters using the FRG [81]. This shows that the moat regime is in the spacelike regime, with a significant width for the spectral density. In future work, we will extend our results to  $p \neq 0$ . It will be interesting to see if a van Hove singularity, which is washed out at  $\vec{p} = 0$  by the vertices in Eq. (18), emerges when  $p \neq 0$ . Inevitably, this singularity is smoothed out by the finite width of moatons.

Moat signals like dilepton production and HBT interferometry [67, 68] may be difficult to extract experimentally. However, if the system lasts sufficiently long in the moat regime, given the extremely high luminosity of FAIR, there is strong potential for observing this dramatic signature of a new QCD regime in the near future at the CBM experiment.

### ACKNOWLEDGMENTS

F.R. acknowledges discussions with K. Hayashi, L.P. with G. Markó, and S.T.S. with I. Stewart. As we were finishing this work, we also had discussions with K. Hayashi and Y. Tsue. Z.N. was supported by a Leverhulme Trust

International Professorship grant number LIP-202-014 at Oxford. R.D.P. is supported by the U.S. Department of Energy under contract DE-SC0012704, and thanks the Alexander v. Humboldt Foundation for their support. L.P., F.R. and M.W. are supported by the Deutsche Forschungsgemeinschaft (DFG, German Research Foundation) through the Collaborative Research Center TransRegio CRC-TR 211 “Strong- interaction matter under extreme conditions” – project number 315477589 – TRR 211. M.W. acknowledges the support of the Helmholtz Graduate School for Hadron and Ion Research. L.P. acknowledges the support of the Giersch Foundation. S.T.S. was supported by the U.S. Department of Energy, Office of Science, Office of Nuclear Physics from DE-SC0011090; the U.S. National Science Foundation through a Graduate Research Fellowship under Grant No. 1745302; fellowships from the MIT Physics Department and School of Science; and the Hoffman Distinguished Postdoctoral Fellowship through the LDRD Program of Los Alamos National Laboratory under Project 20240786PRD1. Los Alamos National Laboratory is operated by Triad National Security, LLC, for the National Nuclear Security Administration of the U.S. Department of Energy (Contract Nr. 892332188CNA000001).

- 
- [1] A. Bazavov et al. (HotQCD), Chiral crossover in QCD at zero and non-zero chemical potentials, *Phys. Lett. B* **795**, 15 (2019), [arXiv:1812.08235 \[hep-lat\]](#).
- [2] S. Borsanyi, Z. Fodor, J. N. Guenther, R. Kara, S. D. Katz, P. I. Parotto, A. Pasztor, C. Ratti, and K. K. Szabo, QCD Crossover at Finite Chemical Potential from Lattice Simulations, *Phys. Rev. Lett.* **125**, 052001 (2020), [arXiv:2002.02821 \[hep-lat\]](#).
- [3] M. Asakawa and K. Yazaki, Chiral Restoration at Finite Density and Temperature, *Nucl. Phys.* **A504**, 668 (1989).
- [4] M. A. Stephanov, K. Rajagopal, and E. V. Shuryak, Signatures of the tricritical point in QCD, *Phys. Rev. Lett.* **81**, 4816 (1998), [arXiv:hep-ph/9806219 \[hep-ph\]](#).
- [5] M. A. Stephanov, K. Rajagopal, and E. V. Shuryak, Event-by-event fluctuations in heavy ion collisions and the QCD critical point, *Phys. Rev.* **D60**, 114028 (1999), [arXiv:hep-ph/9903292 \[hep-ph\]](#).
- [6] P. Parotto, M. Bluhm, D. Mroczek, M. Nahrgang, J. Noronha-Hostler, K. Rajagopal, C. Ratti, T. Schäfer, and M. Stephanov, QCD equation of state matched to lattice data and exhibiting a critical point singularity, *Phys. Rev. C* **101**, 034901 (2020), [arXiv:1805.05249 \[hep-ph\]](#).
- [7] A. Bzdak, S. Esumi, V. Koch, J. Liao, M. Stephanov, and N. Xu, Mapping the Phases of Quantum Chromodynamics with Beam Energy Scan, *Phys. Rept.* **853**, 1 (2020), [arXiv:1906.00936 \[nucl-th\]](#).
- [8] W.-j. Fu, J. M. Pawłowski, and F. Rennecke, The QCD phase structure at finite temperature and density, *Physical Review D* **101**, 054032 (2020), [arxiv:1909.02991](#).
- [9] F. Gao and J. M. Pawłowski, QCD phase structure from functional methods, *Phys. Rev. D* **102**, 034027 (2020), [arXiv:2002.07500 \[hep-ph\]](#).
- [10] F. Gao and J. M. Pawłowski, Chiral phase structure and critical end point in QCD, *Physics Letters B* **820**, 136584 (2021), 2010.13705 [\[hep-ph, physics:hep-th\]](#).
- [11] P. J. Gunkel and C. S. Fischer, Locating the critical endpoint of QCD: Mesonic backcoupling effects, *Phys. Rev. D* **104**, 054022 (2021), [arXiv:2106.08356 \[hep-ph\]](#).
- [12] G. Basar, QCD critical point, Lee-Yang edge singularities, and Padé resummations, *Phys. Rev. C* **110**, 015203 (2024), [arXiv:2312.06952 \[hep-th\]](#).
- [13] D. A. Clarke, P. Dimopoulos, F. Di Renzo, J. Goswami, C. Schmidt, S. Singh, and K. Zambello, Searching for the QCD critical endpoint using multi-point Padé approximations, (2024), [arXiv:2405.10196 \[hep-lat\]](#).
- [14] To be more precise, the critical mode is a mixture between the  $\sigma$ , the  $\omega^0$  meson and the Polyakov loops [58].
- [15] J. Braun, B. Klein, and P. Piasecki, On the scaling behavior of the chiral phase transition in QCD in finite and infinite volume, *Eur. Phys. J. C* **71**, 1576 (2011), [arXiv:1008.2155 \[hep-ph\]](#).
- [16] B. J. Schaefer and M. Wagner, QCD critical region and higher moments for three flavor models, *Phys. Rev. D* **85**, 034027 (2012), [arXiv:1111.6871 \[hep-ph\]](#).
- [17] F. Gao and J. M. Pawłowski, Phase structure of (2+1)-flavor QCD and the magnetic equation of state, *Phys. Rev. D* **105**, 094020 (2022), [arXiv:2112.01395 \[hep-ph\]](#).
- [18] W.-j. Fu, X. Luo, J. M. Pawłowski, F. Rennecke, and S. Yin, Ripples of the QCD Critical Point, (2023), [arXiv:2308.15508 \[hep-ph\]](#).
- [19] J. Bernhardt and C. S. Fischer, QCD phase transitions in the light quark chiral limit, *Phys. Rev. D* **108**, 114018

- (2023), [arXiv:2309.06737 \[hep-ph\]](#).
- [20] J. Braun et al., Soft modes in hot QCD matter, (2023), [arXiv:2310.19853 \[hep-ph\]](#).
- [21] Y. Lu, F. Gao, Y.-X. Liu, and J. M. Pawłowski, QCD equation of state and thermodynamic observables from computationally minimal Dyson-Schwinger equations, *Phys. Rev. D* **110**, 014036 (2024), [arXiv:2310.18383 \[hep-ph\]](#).
- [22] A. Yoshimori, A new type of antiferromagnetic structure, *J. Phys. Soc. Jpn.* **14**, 805 (1959).
- [23] R. M. Hornreich, M. Luban, and S. Shtrikman, Critical behavior at the onset of  $\vec{k}$ -space instability on the  $\lambda$  line, *Phys. Rev. Lett.* **35**, 1678 (1975).
- [24] M. Seul and D. Andelman, Domain shapes and patterns: The phenomenology of modulated phases, *Science* **267**, 476 (1995).
- [25] S. Chakrabarty and Z. Nussinov, Modulation and correlations lengths in systems with competing interactions: new exponents and other universal features, *Physical Review B* **84**, 144402 (2011).
- [26] S. Chakrabarty, V. Dobrosavljevic, A. Seidel, and Z. Nussinov, Universality of modulation length (and time) exponents, *Physical Review E* **86**, 041132 (2012).
- [27] This also includes models of magnetic materials [22–24, 82], elastic stressed systems [83], liquid crystals [84, 85], chemical mixtures and membranes [24], and general Ginzburg-Landau theories describing competing orders [86]. In these and numerous other arenas, the interplay between the varying order gradient terms leads to low energy states which may obtain their minima at finite wave-vectors. The resulting moat-type structures underlie basic aspects of crystallization [87, 88], superconductors in external magnetic fields [89–91], quantum Hall systems [28, 92–97], and countless others.
- [28] S. Pu, A. C. Balma, J. Taylor, E. Fradkin, and Z. Papic, Microscopic model for fractional quantum hall nematics, *Phys. Rev. Lett.* **132**, 236503 (2024).
- [29] T. A. Sedrakyan, L. I. Glazman, and A. Kamenev, Absence of bose condensation on lattices with moat bands, *Phys. Rev. B* **89**, 201112(R) (2014).
- [30] M. A. Schindler, S. T. Schindler, L. Medina, and M. C. Ogilvie, Universality of Pattern Formation, *Phys. Rev. D* **102**, 114510 (2020), [arXiv:1906.07288 \[hep-lat\]](#).
- [31] P. N. Meisinger and M. C. Ogilvie, PT Symmetry in Classical and Quantum Statistical Mechanics, *Phil. Trans. Roy. Soc. Lond. A* **371**, 20120058 (2013), [arXiv:1208.5077 \[math-ph\]](#).
- [32] M. A. Schindler, S. T. Schindler, and M. C. Ogilvie, PT symmetry, pattern formation, and finite-density QCD, *J. Phys.: Conf. Ser.* **2038**, 10.1088/1742-6596/2038/1/012022 (2021), [arXiv:2106.07092 \[hep-lat\]](#).
- [33] C. M. Bender and S. Boettcher, Real spectra in nonHermitian Hamiltonians having PT symmetry, *Phys. Rev. Lett.* **80**, 5243 (1998), [arXiv:physics/9712001](#).
- [34] C. M. Bender, P. E. Dorey, C. Dunning, A. Fring, D. W. Hook, H. F. Jones, S. Kuzhel, G. Lévai, and R. Tateo, *PT Symmetry* (WSP, 2019).
- [35] C. M. Bender and D. W. Hook, PT-symmetric quantum mechanics, (2023), [arXiv:2312.17386 \[quant-ph\]](#).
- [36] J. Stephenson, Ising Model with Antiferromagnetic Next-Nearest-Neighbor Coupling: Spin Correlations and Disorder Points, *Physical Review B* **1**, 4405 (1970).
- [37] A. L. Fetter and J. D. Walecka, *Quantum theory of many-particle systems* (Courier Corporation, 2012).
- [38] M. Thies and K. Urlichs, Revised phase diagram of the Gross-Neveu model, *Phys. Rev. D* **67**, 125015 (2003), [arXiv:hep-th/0302092](#).
- [39] G. Basar and G. V. Dunne, A Twisted Kink Crystal in the Chiral Gross-Neveu model, *Phys. Rev. D* **78**, 065022 (2008), [arXiv:0806.2659 \[hep-th\]](#).
- [40] G. Basar, G. V. Dunne, and M. Thies, Inhomogeneous Condensates in the Thermodynamics of the Chiral NJL(2) model, *Phys. Rev. D* **79**, 105012 (2009), [arXiv:0903.1868 \[hep-th\]](#).
- [41] J. Lenz, L. Pannullo, M. Wagner, B. Wellegehausen, and A. Wipf, Inhomogeneous phases in the Gross-Neveu model in 1+1 dimensions at finite number of flavors, *Phys. Rev. D* **101**, 094512 (2020), [arXiv:2004.00295 \[hep-lat\]](#).
- [42] J. J. Lenz, M. Mandl, and A. Wipf, Inhomogeneities in the two-flavor chiral Gross-Neveu model, *Phys. Rev. D* **105**, 034512 (2022), [arXiv:2109.05525 \[hep-lat\]](#).
- [43] J. J. Lenz and M. Mandl, Remnants of large- $N_f$  inhomogeneities in the 2-flavor chiral Gross-Neveu model, *PoS LATTICE2021*, 415 (2022), [arXiv:2110.12757 \[hep-lat\]](#).
- [44] C. Nonaka and K. Horie, Inhomogeneous phases in the chiral Gross-Neveu model on the lattice, *PoS LATTICE2021*, 150 (2022), [arXiv:2112.02261 \[hep-lat\]](#).
- [45] L. Pannullo, Inhomogeneous condensation in the Gross-Neveu model in noninteger spatial dimensions  $1 \leq d < 3$ , *Phys. Rev. D* **108**, 036022 (2023), [arXiv:2306.16290 \[hep-ph\]](#).
- [46] A. Koenigstein and L. Pannullo, Inhomogeneous condensation in the Gross-Neveu model in noninteger spatial dimensions  $1 \leq d < 3$ . II. Nonzero temperature and chemical potential, *Phys. Rev. D* **109**, 056015 (2024), [arXiv:2312.04904 \[hep-ph\]](#).
- [47] A. Koenigstein, L. Pannullo, S. Rechenberger, M. J. Steil, and M. Winstel, Detecting inhomogeneous chiral condensation from the bosonic two-point function in the (1 + 1)-dimensional Gross-Neveu model in the mean-field approximation\*, *J. Phys. A* **55**, 375402 (2022), [arXiv:2112.07024 \[hep-ph\]](#).
- [48] D. Nickel, Inhomogeneous phases in the Nambu-Jona-Lasinio and quark-meson model, *Physical Review D* **80**, 074025 (2009), [arxiv:0906.5295](#).
- [49] M. Buballa and S. Carignano, Inhomogeneous chiral symmetry breaking in dense neutron-star matter, *Eur. Phys. J. A* **52**, 57 (2016), [arXiv:1508.04361 \[nucl-th\]](#).
- [50] T.-G. Lee, E. Nakano, Y. Tsue, T. Tatsumi, and B. Friman, Landau-Peierls instability in a Fulde-Ferrell type inhomogeneous chiral condensed phase, *Phys. Rev. D* **92**, 034024 (2015), [arXiv:1504.03185 \[hep-ph\]](#).
- [51] Y. Hidaka, K. Kamikado, T. Kanazawa, and T. Noumi, Phonons, pions and quasi-long-range order in spatially modulated chiral condensates, *Phys. Rev. D* **92**, 034003 (2015), [arXiv:1505.00848 \[hep-ph\]](#).
- [52] M. Buballa and S. Carignano, Inhomogeneous chiral phases away from the chiral limit, *Phys. Lett. B* **791**, 361 (2019), [arXiv:1809.10066 \[hep-ph\]](#).
- [53] S. Carignano and M. Buballa, Inhomogeneous chiral condensates in three-flavor quark matter, *Phys. Rev. D* **101**, 014026 (2020), [arXiv:1910.03604 \[hep-ph\]](#).
- [54] L. Pannullo, M. Wagner, and M. Winstel, Regularization effects in the Nambu-Jona-Lasinio model: Strong scheme dependence of inhomogeneous phases and persistence of the moat regime, (2024), [arXiv:2406.11312 \[hep-ph\]](#).
- [55] T. F. Motta, J. Bernhardt, M. Buballa, and C. S. Fischer,

- Inhomogeneous instabilities at large chemical potential in a rainbow-ladder QCD model, (2024), [arXiv:2406.00205 \[hep-ph\]](#).
- [56] H. Nishimura, M. C. Ogilvie, and K. Pangeni, Complex saddle points in QCD at finite temperature and density, *Phys. Rev. D* **90**, 045039 (2014), [arXiv:1401.7982 \[hep-ph\]](#).
- [57] H. Nishimura, M. C. Ogilvie, and K. Pangeni, Complex Saddle Points and Disorder Lines in QCD at finite temperature and density, *Phys. Rev. D* **91**, 054004 (2015), [arXiv:1411.4959 \[hep-ph\]](#).
- [58] M. Haensch, F. Rennecke, and L. von Smekal, Medium induced mixing, spatial modulations, and critical modes in QCD, *Phys. Rev. D* **110**, 036018 (2024), [arXiv:2308.16244 \[hep-ph\]](#).
- [59] H. Nishimura, M. C. Ogilvie, and K. Pangeni, Complex spectrum of finite-density lattice QCD with static quarks at strong coupling, *Phys. Rev. D* **93**, 094501 (2016), [arXiv:1512.09131 \[hep-lat\]](#).
- [60] H. Nishimura, M. C. Ogilvie, and K. Pangeni, Liquid-Gas Phase Transitions and  $CK$  Symmetry in Quantum Field Theories, *Phys. Rev. D* **95**, 076003 (2017), [arXiv:1612.09575 \[hep-th\]](#).
- [61] M. Winstel, Spatially oscillating correlation functions in (2+1)-dimensional four-fermion models: The mixing of scalar and vector modes at finite density, *Phys. Rev. D* **110**, 034008 (2024), [arXiv:2403.07430 \[hep-ph\]](#).
- [62] In perturbative QCD with massless quarks, Friedel oscillations arise as an oscillatory function times a power law fall-off.[98].
- [63] R. D. Pisarski, V. V. Skokov, and A. M. Tsvetik, Fluctuations in cool quark matter and the phase diagram of Quantum Chromodynamics, *Phys. Rev. D* **99**, 074025 (2019), [arXiv:1801.08156 \[hep-ph\]](#).
- [64] R. D. Pisarski, A. M. Tsvetik, and S. Valgushev, How transverse thermal fluctuations disorder a condensate of chiral spirals into a quantum spin liquid, *Phys. Rev. D* **102**, 016015 (2020), [arXiv:2005.10259 \[hep-ph\]](#).
- [65] M. Winstel and S. Valgushev, Lattice study of disordering of inhomogeneous condensates and the Quantum Pion Liquid in effective  $O(N)$  model, in *Excited QCD 2024 Workshop* (2024) [arXiv:2403.18640 \[hep-lat\]](#).
- [66] R. D. Pisarski, F. Rennecke, A. Tsvetik, and S. Valgushev, The Lifshitz Regime and its Experimental Signals, *Nucl. Phys. A* **1005**, 121910 (2021), [arXiv:2005.00045 \[nucl-th\]](#).
- [67] R. D. Pisarski and F. Rennecke, Signatures of Moat Regimes in Heavy-Ion Collisions, *Phys. Rev. Lett.* **127**, 152302 (2021), [arXiv:2103.06890 \[hep-ph\]](#).
- [68] F. Rennecke, R. D. Pisarski, and D. H. Rischke, Particle interferometry in a moat regime, *Phys. Rev. D* **107**, 116011 (2023), [arXiv:2301.11484 \[hep-ph\]](#).
- [69] K. Fukushima, Y. Hidaka, K. Inoue, K. Shigaki, and Y. Yamaguchi, Hanbury-Brown–Twiss signature for clustered substructures probing primordial inhomogeneity in hot and dense QCD matter, *Phys. Rev. C* **109**, L051903 (2024), [arXiv:2306.17619 \[hep-ph\]](#).
- [70] K. Hayashi and Y. Tsue, Modified dilepton production rate from charged pion-pair annihilation in the inhomogeneous chiral condensed phase, (2024), [arXiv:2407.08523 \[hep-ph\]](#).
- [71] I. Balog, H. Chaté, B. Delamotte, M. Marohnic, and N. Wschebor, Convergence of Nonperturbative Approximations to the Renormalization Group, *Phys. Rev. Lett.* **123**, 240604 (2019), [arXiv:1907.01829 \[cond-mat.stat-mech\]](#).
- [72] On a lattice, the continuum limit  $k^4$  term is replaced by a squared lattice Laplacian corresponding to competing nearest and next nearest neighbor interactions.
- [73] If higher derivative terms dominate with negative coefficients, then even if  $Z > 0$ , it is possible that  $E(p)$  about  $p = 0$  is a local minimum, but that the global minimum of  $E(p)$  is at  $p \neq 0$ .
- [74] This occurs, e.g., for a roton, where  $p = 0$  is the global minimum, but there is a local minimum for one or more  $p_{\text{roton}} \neq 0$ .
- [75] L. D. McLerran and T. Toimela, Photon and Dilepton Emission from the Quark - Gluon Plasma: Some General Considerations, *Phys. Rev. D* **31**, 545 (1985).
- [76] H. B. O’Connell, B. C. Pearce, A. W. Thomas, and A. G. Williams,  $\rho - \omega$  mixing, vector meson dominance and the pion form-factor, *Prog. Part. Nucl. Phys.* **39**, 201 (1997), [arXiv:hep-ph/9501251](#).
- [77] R. Rapp and J. Wambach, Chiral symmetry restoration and dileptons in relativistic heavy ion collisions, *Adv. Nucl. Phys.* **25**, 1 (2000), [arXiv:hep-ph/9909229](#).
- [78] R. Rapp and H. van Hees, Thermal Electromagnetic Radiation in Heavy-Ion Collisions, *Eur. Phys. J. A* **52**, 257 (2016), [arXiv:1608.05279 \[hep-ph\]](#).
- [79] R. Rapp, Electric Conductivity of QCD Matter and Dilepton Spectra in Heavy-Ion Collisions, (2024), [arXiv:2406.14656 \[hep-ph\]](#).
- [80] E. Braaten, R. D. Pisarski, and T.-C. Yuan, Production of Soft Dileptons in the Quark - Gluon Plasma, *Phys. Rev. Lett.* **64**, 2242 (1990).
- [81] W.-J. Fu, J. M. Pawłowski, R. D. Pisarski, F. Rennecke, R. Wen, and S. Yin, The moat regime in QCD (2024), work in progress.
- [82] W. Selke, The anmi model- theoretical analysis and experimental application, *Physics Reports* **170**, 213 (1988).
- [83] A. Aharony and A. D. Bruce, Lifshitz-point critical and tricritical behavior in anisotropically stressed perovskites, *Phys. Rev. Lett.* **42**, 462 (1979).
- [84] E. Abrahams and I. E. Dzyaloshinskii, A possible lifshitz point for  $\text{ttf-tcnq}$ , *Solid State Commun.* **23**, 883 (1977).
- [85] J. V. Selinger, Director deformations, geometric frustration, and modulated phases in liquid crystals, *Annual Review of Condensed Matter Physics* **13**, 49 (2022).
- [86] A. Nussinov, I. Vekhter, and A. V. Balatsky, onuniform glassy electronic phases from competing local orders, *Physical Review B* **79**, 165122 (2009).
- [87] S. A. Brazovskii, Phase transition of an isotropic system to a nonuniform state, *Zh. Eksp. Teor. Fiz.* **68**, 175 (1975).
- [88] S. A. Brazovskii, I. E. Dzyaloshinskii, and A. R. Muratov, Theory of weak crystallization, *Sov. Phys. JETP* **66**, 625 (1987).
- [89] P. Fulde and R. A. Ferrell, Superconductivity in a strong spin-exchange field, *Phys. Rev.* **135**, A550 (1964).
- [90] A. I. Larkin and Y. N. Ovchinnikov, Nonuniform state of superconductors, *Zh. Eksp. Teor. Fiz.* **47**, 1136 (1964).
- [91] A. I. Larkin and Y. N. Ovchinnikov, Inhomogeneous state of superconductors, *Sov. Phys. JETP* **20**, 762 (1965).
- [92] M. P. Lilly, K. B. Cooper, J. P. Eisenstein, L. N. Pfeiffer, and K. W. West, Evidence for an anisotropic state of two-dimensional electrons in high landau levels, *Phys. Rev. Lett.* **82**, 394 (1999).
- [93] E. Fradkin and S. A. Kivelson, Liquid-crystal phases of quantum hall systems, *Phys. Rev. B* **59**, 8065 (1999).

- [94] M. M. Fogler, A. A. Koulakov, and B. I. Shklovskii, Ground state of a two-dimensional electron liquid in a weak magnetic field, *Phys. Rev. B* **54**, 1853 (1996).
- [95] R. Moessner and J. T. Chalker, Exact results for interacting electrons in high Landau levels, *Phys. Rev. B* **54**, 5006 (1996).
- [96] A. A. Koulakov, M. M. Fogler, and B. I. Shklovskii, Charge density wave in two-dimensional electron liquid in weak magnetic field, *Phys. Rev. Lett.* **76**, 499 (1996).
- [97] R. Du, D. Tsui, H. Stormer, L. Pfeiffer, K. Baldwin, and K. West, Strongly anisotropic transport in higher two-dimensional Landau levels, *Solid State Communications* **109**, 389 (1999).
- [98] J. I. Kapusta and T. Toimela, Friedel Oscillations in Relativistic QED and QCD, *Phys. Rev. D* **37**, 3731 (1988).



## Appendix A: Supplemental material

To illustrate how the van Hove singularity is smoothed out by correctly imposing gauge invariance, in Fig. 3 we compute the dilepton production in two different ways. Both use Eq. (2) at  $p = 0$ , and the dispersion relations in Fig. 2. Solid lines represent the correct result, where both the quadratic and quartic terms are gauged; dashed lines are the result where only the quadratic term is gauged. For the former, the threshold behavior of pions with a mass is smooth, like normal pions; for the latter, there are van Hove singularities, which are thus unphysical at  $p = 0$ . Neglecting gauge invariance for higher order terms is equivalent to taking  $M \rightarrow \infty$  for the photon- $\phi$ - $\phi$  vertex,  $\Gamma^\mu$ . Such a vertex does not satisfy the Ward identity of Eq. (9), so the photon self energy,  $\Pi^{\mu\nu}$  is not transverse,  $P^\mu \Pi^{\mu\nu} \neq 0$ . As described in the main part of the manuscript, the correct vertex structure near threshold, Eq. (18), smooths out the van Hove singularity, and leads to the observed enhancement of the dilepton production.

We note that Ref. [70] did not use a gauge invariant form for the higher order derivative terms. Thus their  $\Gamma^\mu$  does not satisfy the Ward identity of Eq. (9), and the associated photon self energy is not transverse. Moreover, the new gauge invariant operators to sixth order in the mass dimension, Eqs. (3)-(6), were not considered in Ref. [70].

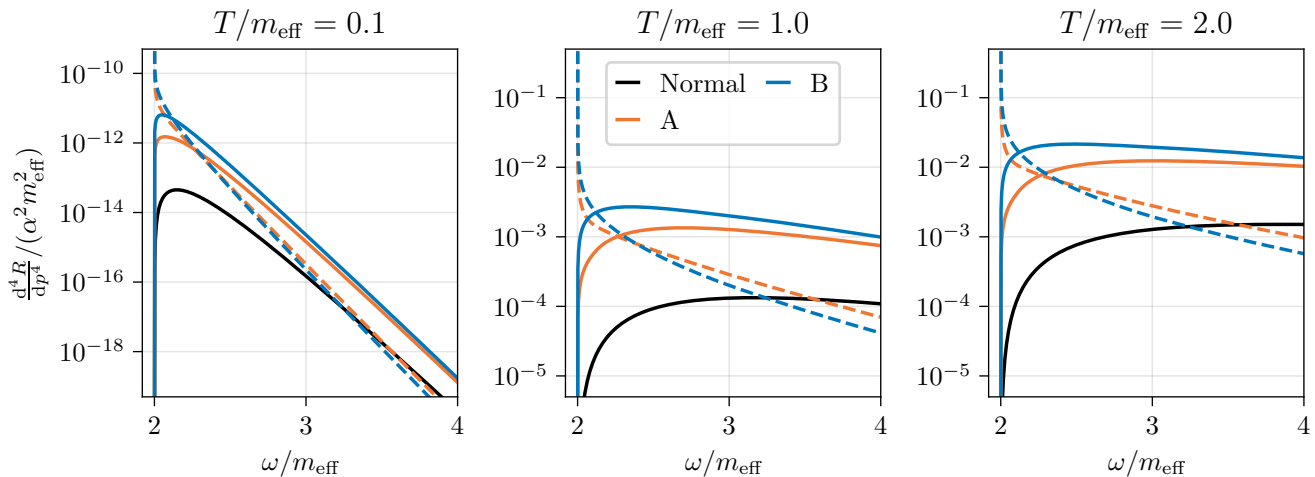


FIG. 3. Dilepton production rate in Eq. (2) as a function of  $\omega$  at  $T/m_{\text{eff}} = 0.1, 0.5, 1.0$ , for the dispersion relations in Fig. 2, at  $\vec{p} = 0$ . Solid lines represent the correct result; dashed lines are the result where only the quadratic term is gauged.